Research Square

Preprints are preliminary reports that have not undergone peer review. They should not be considered conclusive, used to inform clinical practice, or referenced by the media as validated information.

Green-Synthesized Co_3O_4 Nanoparticles from Thyme, Teucrium oliverianum, and Cercis siliquastrum: Enhanced Photocatalytic Degradation of Methylene Blue

Khelan S. Najmaldeen
University of Garmian

Dilan Nawzad Mamakhan
delan.nawzad@garmian.edu.krd

University of Garmian

Research Article

Keywords: Teucrium oliverianum, Thyme, Cercis siliquastrum, Co3O4 NPs, photocatalytic activity, methylene blue

Posted Date: August 6th, 2026

DOI: https://doi.org/10.21203/rs.3.rs-10438934/v1

License: This work is licensed under a Creative Commons Attribution 4.0 International License. Read Full License

Additional Declarations: No competing interests reported.

Version of Record: A version of this preprint was published at Reaction Kinetics, Mechanisms and Catalysis on September 3rd, 2026. See the published version at https://doi.org/10.1007/s11144-026-03237-3.

Green-Synthesized Co_3O_4 Nanoparticles from Thyme, *Teucrium oliverianum*, and *Cercis siliquastrum*: Enhanced Photocatalytic Degradation of Methylene Blue

Khelan S. Najmaldeen[a], Dilan Nawzad Mamakhan[a]

[a] *Chemistry Department, Education College, University of Garmian, Kalar City, Sulaimaniyah, Kurdistan Region, Iraq.*

Corresponding author: delan.nawzad@garmian.edu.krd

khelan.najmaldeen@garmian.edu.krd

Abstract

Industrial dye contamination remains a critical environmental challenge, necessitating the development of efficient, sustainable, and cost-effective wastewater treatment technologies. In this study, green-synthesized cobalt oxide nanoparticles (Co_3O_4 NPs) prepared from *Teucrium oliverianum*, *Thymus vulgaris* (thyme), and *Cercis siliquastrum* leaf extracts were investigated as photocatalysts for the degradation of methylene blue under UV irradiation through a photo-contact electrification mechanism. Their performance was systematically compared with chemically synthesized Co_3O_4 nanoparticles and catalyst-free photolysis. The synthesized nanoparticles were comprehensively characterized using UV–Vis spectroscopy, FTIR, XRD, FE-SEM, and TEM. The green-synthesized Co_3O_4 NPs exhibited markedly enhanced photocatalytic activity, achieving dye degradation efficiencies of 98.99%, 95.42%, and 95.30% for *C. siliquastrum*, thyme, and *T. oliverianum*, respectively, compared with 89.64% for chemically synthesized Co_3O_4 NPs and 25.98% for UV treatment alone. The superior performance of the biosynthesized nanoparticles is attributed to their smaller particle size, improved morphology, and the presence of phytochemical-derived capping agents that promote charge separation and increase the availability of active catalytic sites. These findings demonstrate that plant-mediated Co_3O_4 nanoparticles represent an environmentally benign and highly effective photocatalyst for dye degradation, offering a promising strategy for the sustainable treatment of dye-contaminated wastewater.

Keywords: *Teucrium oliverianum*; Thyme; *Cercis siliquastrum*; Co_3O_4 NPs; photocatalytic activity; methylene blue.

Graphical abstract

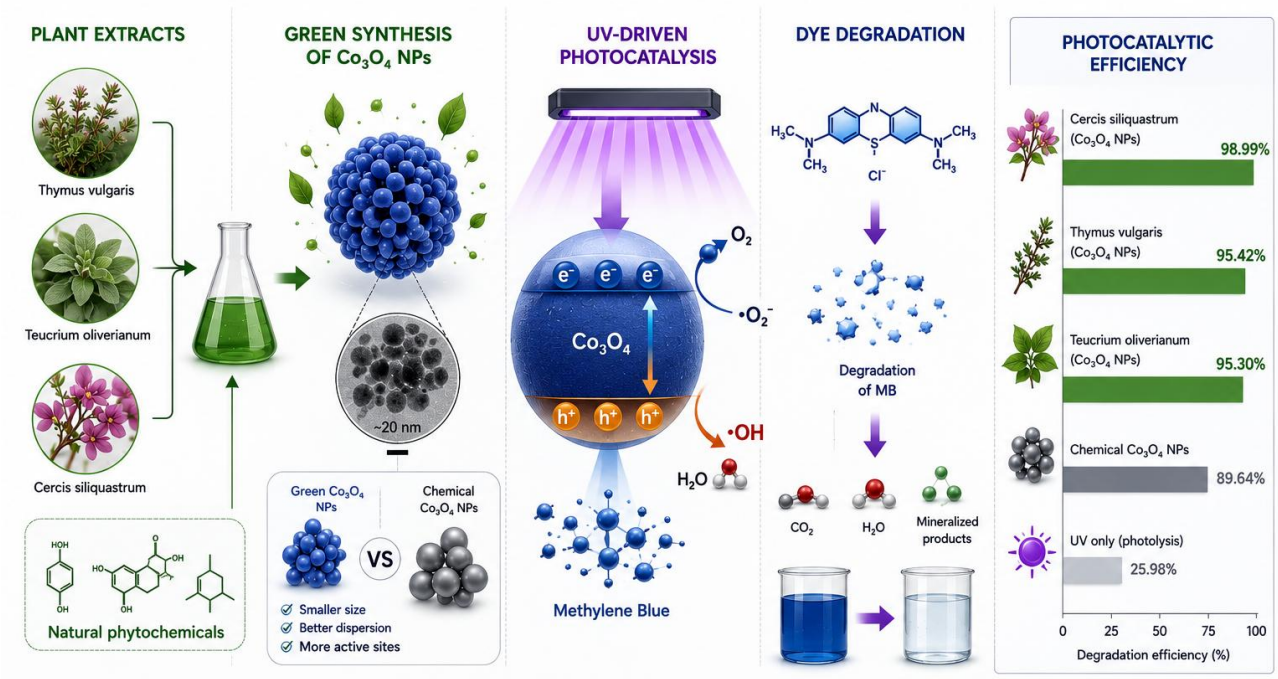

1. Introduction

Rapid industrialization, urbanization, and population growth have significantly increased global water pollution, posing serious threats to ecosystems and public health. According to the World Health Organization (WHO), approximately 2.3 million deaths annually are associated with waterborne diseases caused by contaminated water [1][2]. Among the major pollutants, synthetic dyes released from textile, paper, leather, and printing industries are particularly concerning because of their persistence, toxicity, and resistance to biodegradation [3][4][5][6]. Methylene blue (MB), a widely used cationic dye, reduces light penetration, inhibits photosynthesis, and adversely affects aquatic organisms even at low concentrations, making its efficient removal from wastewater an important environmental challenge [7][8][9][10].

Various physical, chemical, and biological methods have been developed for dye removal; however, photocatalytic degradation has emerged as one of the most effective and environmentally sustainable approaches [11][12][13][14]. Upon light irradiation, semiconductor photocatalysts generate electron–hole pairs that produce reactive oxygen species (ROS), such as hydroxyl and superoxide radicals, which mineralize organic pollutants into harmless products, including CO_2 and H_2O [15][16][17]. Among photocatalysts, cobalt oxide (Co_3O_4) nanoparticles have attracted considerable attention because of their excellent light absorption, catalytic activity, chemical stability, and visible-light responsiveness [18][19][20][21].

Green synthesis using plant extracts offers a simple, cost-effective, and environmentally friendly alternative to conventional chemical methods. Plant phytochemicals, including flavonoids and polyphenols, act as natural reducing and stabilizing agents, producing nanoparticles with improved stability and tailored physicochemical properties [22][23][24][25][26]. Nevertheless, comparative studies evaluating the influence of different plant extracts on the characteristics and photocatalytic performance of Co_3O_4 nanoparticles remain limited.

In this study, Co_3O_4 nanoparticles were green synthesized using leaf extracts of *Teucrium oliverianum*, *Cercis siliquastrum*, and *Thymus vulgaris* (thyme), and compared with chemically synthesized Co_3O_4 nanoparticles. The

nanoparticles were characterized by UV–Vis, FTIR, XRD, FE-SEM, EDX, and TEM, and their photocatalytic activity toward methylene blue degradation under UV irradiation was evaluated. This study highlights the potential of plant-mediated synthesis to produce efficient and environmentally friendly Co_3O_4 photocatalysts for wastewater treatment.

2. Materials and Methods

2.1. Materials

The precursor materials utilized in this study included cobalt chloride hexahydrate ($CoCl_2.6H_2O$, 98 %), ammonia aqueous (NH_4OH, 28 %). All these chemicals were sourced from Sigma-Aldrich. Deionized water (DI) was used as solvents, and ethanol (C_2H_5OH, ~ 96 %) was utilized as purification of nanoparticles. Methylene blue ($C_{16}H_{18}ClN_3S$) was supplied by Sigma-Aldrich Company (Germany) without additional purification.

2.2. Preparation of leaf extracts

Fresh leafs of Thyme, *Teucrium oliverianum* and *Cercis siliquastrum* were collected from the Salahaddin University campus and thoroughly washed with sterile water to remove impurities. Following a series of cleansing to eliminate any lingering moisture or unwanted contaminants like dirt, dust, pesticides and others, they were then shade-dried for 15 days to eliminate any last traces of moisture [34]. Separately, 30 grams of powdered dried of each leaves were placed in a 500 milliliter glass flask. After adding 200 milliliter of double distilled water (DDW), Subsequently, the paste was heated at 80 °C for one hours to extract the active compounds. Once cooled to room temperature, the mixture was filtered utilizing Whatman filter paper. The filtrate was eventually utilized to synthesis the necessary Co_3O_4 NPs.

2.3. Preparation of Cobalt oxide nanoparticles (Co_3O_4 NPs)

By applying the plant-mediated "green synthesis" technique, which uses various active groups found in plants as reducing ends to create nanoparticles, biogenic Co_3O_4 NPs were created show in the **Figure 1 (a)**. 0.1 mole of cobalt chloride hexahydrate ($CoCl_2.6H_2O$, 98 %) solution was prepared by adding 50 ml of demineralized water. Then, 30 ml of each one aqueous leaf extracts were added to it drop by drop. After 30 minutes of placing it on a magnetic stirrer, the colour shift was noticed. In this reaction, the ammonium hydroxide (NH_4OH, 28 %) solution was added to maintain the required pH (8.11). Later the solution was stirred for 6 hours. To get rid of contaminants, the resulting precipitate was cleaned with ethanol and deionized water before being put into a china plate. A hot air oven was used to dry the precipitates for 12 hours at 80 °C. Beyond drying, the precursor was ground into a fine powder and calcined for five hours at 500 °C [27]. The synthesized nanoparticles were then analyzed utilizing UV–vis spectroscopy. **Figure 1 (b)** show the chemical synthesis of Co_3O_4 NPs, a 0.1 mole of cobalt chloride solution was prepared by adding 50 ml of demineralized water (solution A). Then, 20 ml of ammonium hydroxide (~28 % NH3 base, Sigma-Aldrich) solution was added to 30 ml of dematerialized water (solution B). The solutions A and B were mixed and stirred for 30 minutes. In this reaction, the ammonia (NH_4OH) solution was added to maintain the required pH (8.11). The final solution was stirred for 6h. The obtained precipitate was washed utilizing ethanol and deionized water consequently. Then, the washed material was dried at 80 °C for 12 h in a hot air oven. It was calcined at 500 °C for 5 h [27]. The synthesized nanoparticles were then analyzed utilizing UV–vis spectroscopy.

2.4. Photocatalytic Tests

To measure the MB degradation, a spectrophotometer was used at a maximum wavelength of 664 nm. The degradation (D) for each experiment was calculated utilizing the following formula **Eq.1.**

$$Dye\ removal = \frac{C_o - C_t}{C_o} X\ 100 \qquad \textbf{(1)}$$

Where C_o represents the initial MB concentration (mg/L), whereas C_t denotes its concentration at time 't' (mg/L). The phytosynthesized and chemically Co_3O_4 NPs were utilized for degradation of methylene blue (MB) dye. Seven hundred milliliters of 50 mg/L methylene blue (MB) aqueous solution was utilized for the photocatalytic experiment. 0.75g of the Co_3O_4 NPs were adding to MB aqueous solution and stirred with a magnetic agitator in the darkness for thirty minutes to create adsorption–desorption balance in the mixture of the solution and catalyst before being exposed to 50 W, CHX-FL-A-50W (λ <400 nm) radiation. The UV light was turned on, and After a certain amount of time (30, 60, 90, 120, 150, 180, 210, and 240 minutes), the samples were filtered utilizing centrifugation to settle down the suspended catalyst and then analyzed by Ultraviolet-visible spectrophotometer in the range of 300–800 nm. The extent of MB degradation in the aqueous solution at around 665 nm wavelength was assessed by the absorbance measurements. All the aqueous sample were at natural pH, and all experiments were conducted at 323K, as temperatures around 323 K are commonly encountered in natural environments during summer, especially in regions with high solar exposure. The photocatalytic experiments were carried out in a custom-designed black-box photoreactor equipped with a UV light source positioned 20 cm above the blue solution. A hotplate was placed inside the box to maintain the desired 323 K temperature with stirring 400 rpm. During each experiment, the box was fully sealed to ensure that UV light was evenly distributed across the solution, providing homogeneous irradiation throughout the reaction show in **Figure 1(c)**.

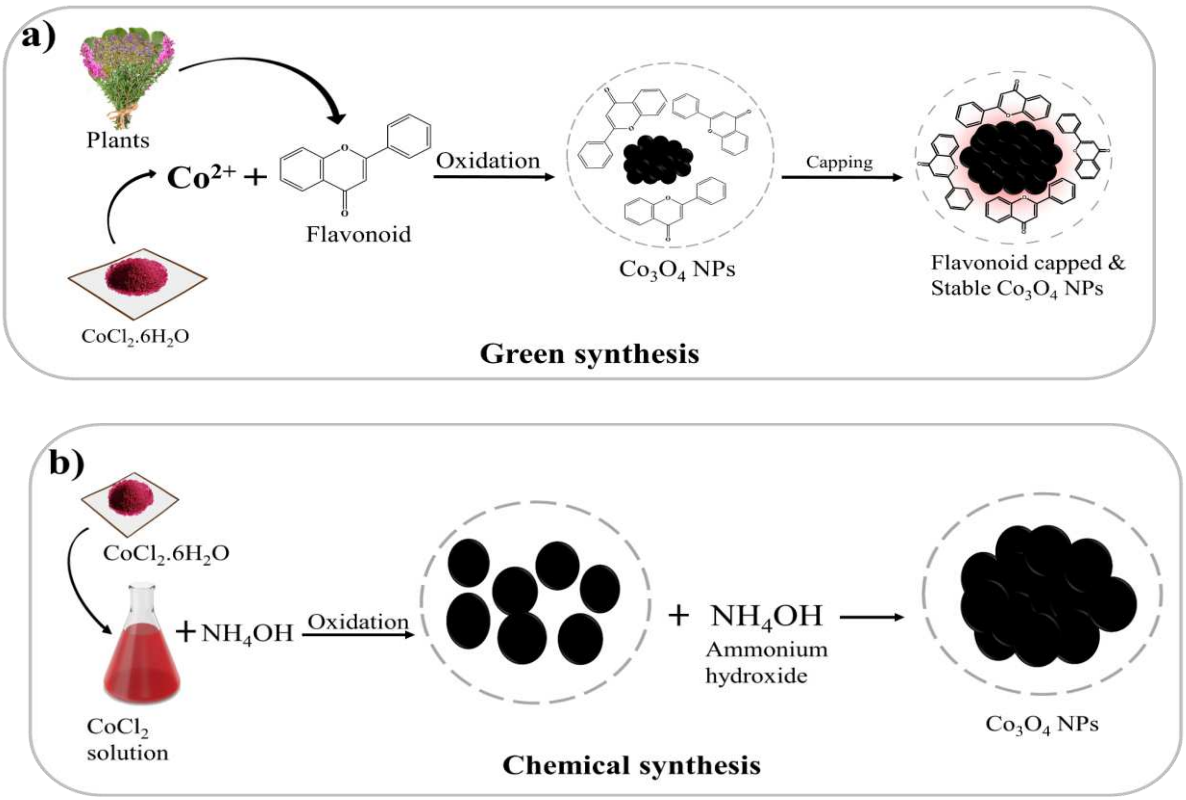

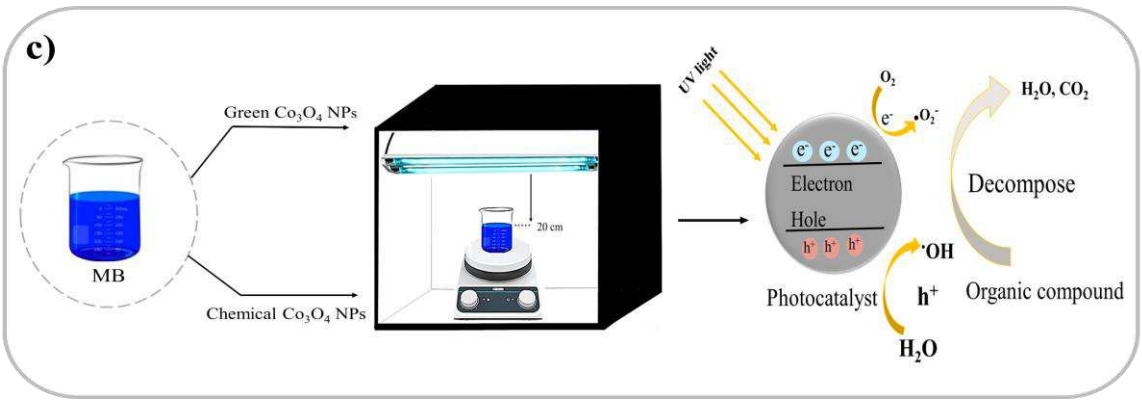

Figure 1. Schematic diagram of green **(a)**, chemical synthesis of Co_3O_4 NPs **(b)**, and **(c)** degradation of methylene blue under UV light (50 W).

2.5. Characterization

The synthesized Co_3O_4 nanoparticles (Co_3O_4 NPs) were comprehensively characterized to evaluate their optical, structural, morphological, and chemical properties. Biosynthesized Co_3O_4 NPs prepared using *Thymus vulgaris*, *Thymus oliverianus*, and *Cercis siliquastrum* extracts, together with chemically synthesized Co_3O_4 NPs, were analyzed by UV–Vis spectroscopy (Shimadzu UV-1900i). Functional groups were identified by FTIR spectroscopy (IRTracer-100, Shimadzu) over the range of 4000–400 cm^{-1}. The crystalline structure was examined by X-ray diffraction (XRD; Rigaku D/MAX 2500V/PC) using Cu Kα radiation (λ = 0.15406 nm) over a 2θ range of 10–70°. Surface morphology and elemental composition were investigated using FE-SEM (Hitachi S-4800) coupled with EDX, while particle size and internal morphology were analyzed by TEM (JEOL TEM-3010). Co^{2+} ion leaching was quantified using ICP-OES (Thermo Scientific iCAP 7600 Duo) to assess catalyst stability.

2.6. Statistical Analysis

All experiments were conducted in triplicate. One-way analysis of variance (ANOVA) was performed using IBM SPSS version 27. The results are reported as mean ± standard deviation (SD). Reproducibility was assessed utilizing the relative standard deviation (RSD %). Data visualization and graph generation were carried out utilizing Origin 2021 software.

3. Results and Discussion

3.1. Spectroscopic Analysis

3.1.1. UV-Vis Spectra and Optical Bandgap

UV-Vis spectroscopy (**Figure 2**) confirmed the successful synthesis of Co_3O_4 nanoparticles (NPs) by both green and chemical methods. The green-synthesized Co_3O_4 NPs exhibited characteristic absorption peak at 506-514 nm, while the chemically synthesized NPs showed peaks at 495-514 nm. respectively. Among the green synthesized samples in **Figure 2(a),** *T. oliverianum* extract produced the highest absorbance intensity, indicating a higher nanoparticle yield and improved crystallinity [28]. This enhanced absorbance is attributed to bioactive phytochemicals, such as flavonoids and polyphenols, which act as reducing and capping agents, promoting efficient nucleation and growth of the nanoparticles.

In contrast, the chemically synthesized Co_3O_4 NPs in **Figure 2(b)** displayed slightly shifted absorption peaks and lower absorbance intensity, likely owing to differences in particle size, crystallinity, and surface defects resulting

from the absence of natural capping agents [27]. Two absorption bands at approximately 514 nm and 762 nm were observed for samples synthesized at pH 8, corresponding to $O^{2-} \rightarrow Co^{2+}$ and $O^{2-} \rightarrow Co^{3+}$ charge transfer transition in the Co_3O_4 nanomaterials, respectively. An additional peak at 276 nm was assigned to the $\pi - \pi^*$ electronic transition between cobalt and oxygen atoms [29]. The calculated optical band gaps were 1.75, 2.43, and 2.05 eV for the Co_3O_4 NPs prepared utilizing *T. oliverianum*, *C. siliquastrum*, and Thyme extracts, respectively **Figure 3**. These band-gap values are associated with oxygen-to-cobalt charge-transfer transitions and are higher than that of chemically synthesized Co_3O_4 (1.52 eV), likely owing to crystal size effects in the nanoparticles [30][31][32][33].

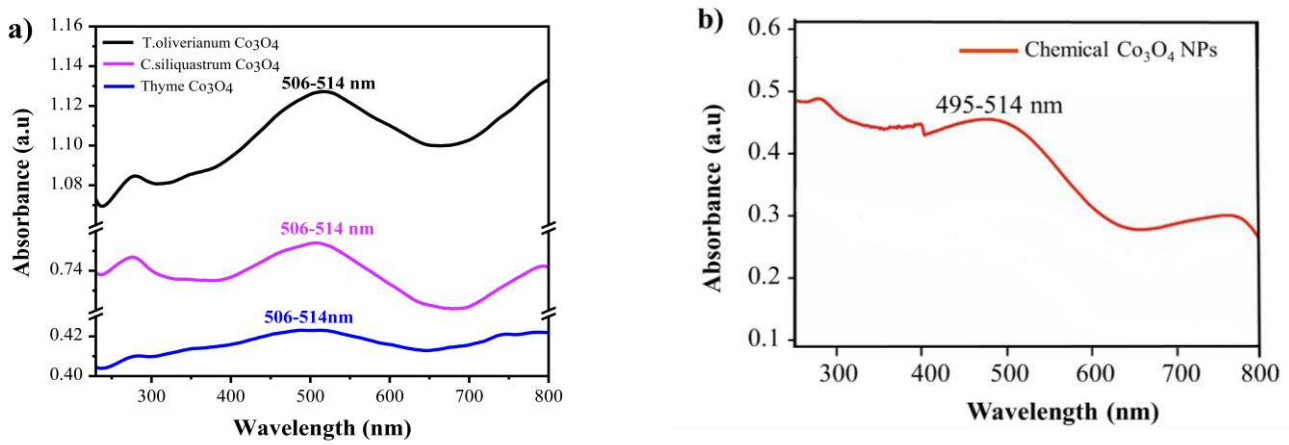

Figure 2. UV–visible spectrum of green synthesized Co_3O_4 NP using T. oliverianum (black line), Thyme (blue line) and C. siliquastrum (pink line) **(a)**, chemically Co_3O_4 NPs **(b)**.

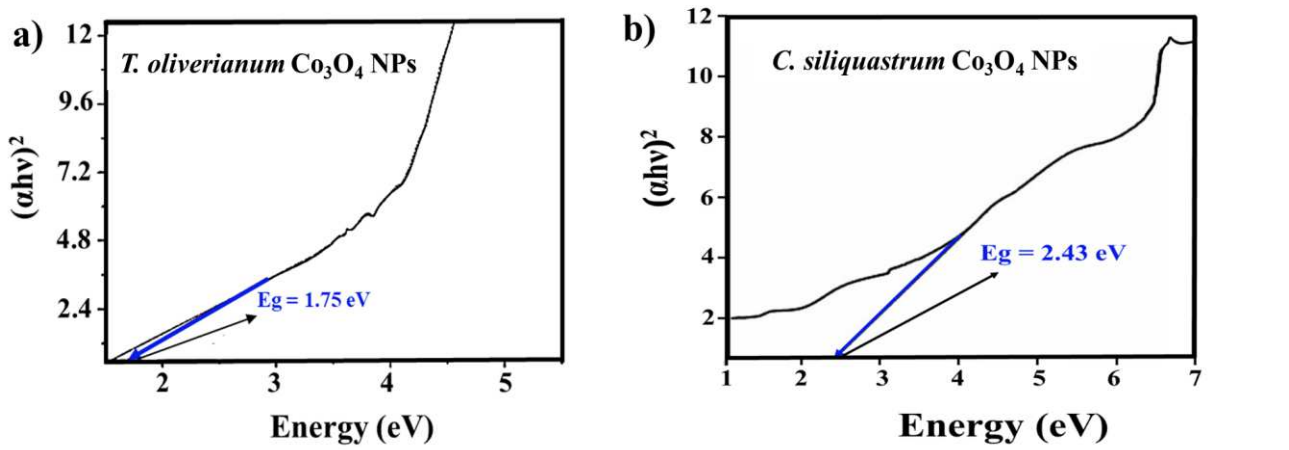

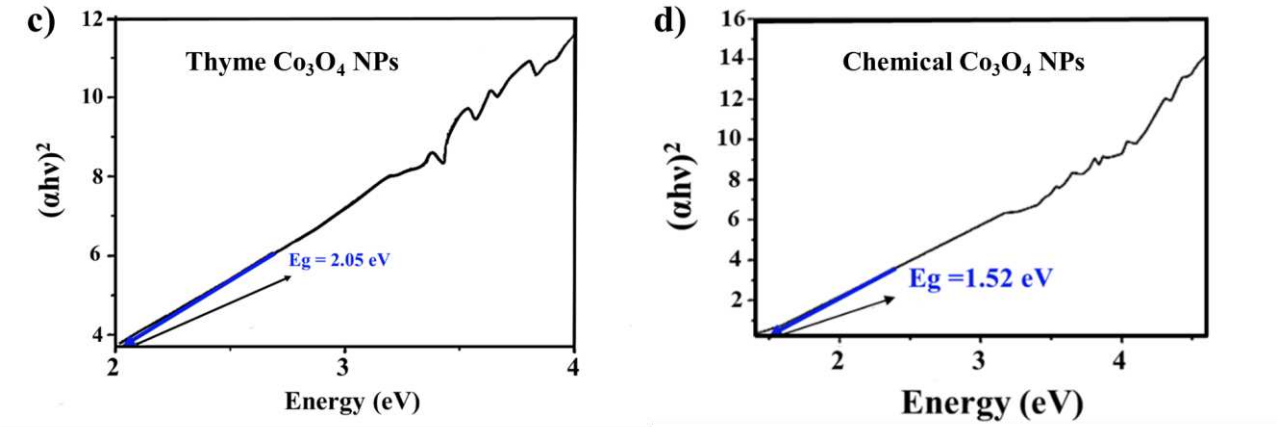

Figure 3. Optical band gap of green Co_3O_4 NPs **(a)** *T. oliverianum*, **(b)** *C. siliquastrum*, **(c)** Thyme, and **(d)** chemically Co_3O_4 NPs.

3.1.2. FTIR Analysis

FTIR analysis was performed to identify the functional groups involved in the interaction between biomolecules and metal oxide nanoparticles in both green and chemically synthesized Co_3O_4 NPs [34]. The FTIR spectrum of green-synthesized Co_3O_4 NPs utilizing Thyme, *T. oliverianum* and *C. siliquastrum* leaf extracts (**Figure 4a**) illustrated a broad band at 3430–3600 cm^{-1}, corresponding to O–H stretching vibrations hydroxyl groups from H_2O molecules and plant phytochemicals [35]. This broad peak may also include N-H stretching vibrations, suggesting the involvement of amine-containing biomolecules in nanoparticles stabilization. Bands at 1600-1650 cm^{-1} were attributed to C=C stretching vibrations of aromatic compounds such as flavonoids, tannins, which may contribute to nanoparticle capping and stabilization. The peak near 1380 cm^{-1} corresponds to C-H bending vibrations, indicating the presence of organic residues [36]. Absorption bands at 1164 cm^{-1} were assigned to C–O-C stretching vibrations, while bands between 850–1150 cm^{-1} were associated with O–C=O and C–O stretching vibrations [37][38]. Characteristic peaks below 800 cm^{-1}, particularly at 665 cm^{-1} and 578 cm^{-1}, were assigned to C–O stretching vibrations, confirming the formation of Co_3O_4 nanoparticles [39].

In contrast, the FTIR spectrum of chemically synthesized Co_3O_4 NPs (**Figure 4b**) exhibited two sharp bands at 584 cm^{-1} and 666 cm^{-1}, corresponding to Co-O and O-Co-O stretching vibrations, respectively [40] [41]. A broad band around 3300 cm^{-1} was attributed to O-H stretching, while weak bands at 1652 and 1619 cm^{-1} were assigned to H-O-H bending vibrations resulting from adsorbed moisture on the sample surface.

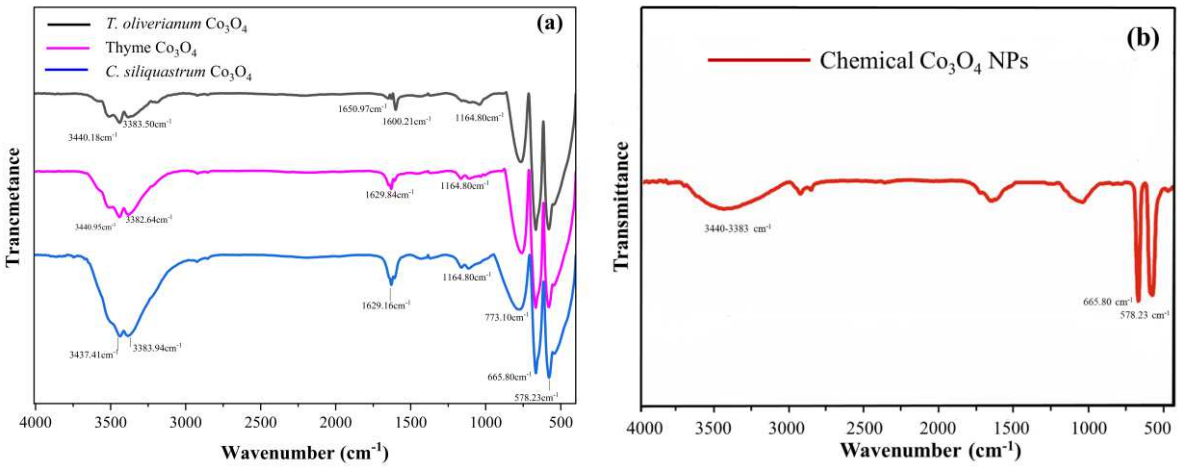

Figure 4. FTIR spectrum of Thyme, *T. oliverianum* and *C. siliquastrum* Co_3O_4 NPs **(a)**, chemical Co_3O_4 NPs **(b)**.

3.1.3. XRD Analysis

X-ray diffraction (XRD) analysis was conducted to investigate the phase composition, crystallinity, and purity of the green-and chemically synthesized Co_3O_4 NPs. As shown in **Figure 5a**, eight characteristic diffraction peaks were observed at 2θ values of 19.22°, 31.52°, 37.12°, 38.84°, 45.11°, 56.00°, 59.71°, and 65.61°, corresponding to the (111), (220), (311), (222), (400), (511), (440), and (442) planes, respectively. These peaks match the face-centered cubic spinel structure of Co_3O_4 (JCPDS file no. 76–1802), confirming the successful formation of phase-pure nanoparticles [42]. Although all samples exhibited the characteristic Co_3O_4 pattern, differences in peak intensity and crystallographic orientation were observed. Chemically synthesized Co_3O_4 NPs showed higher peak intensities, indicating greater crystallinity, however, the (111) reflection was absent, whereas it was present in all green-synthesized samples. This suggests that chemical synthesis may favor specific crystal growth orientations due to rapid and controlled nucleation, while phytochemical-mediated synthesis promotes a more complete crystal structure. The crystallite size was estimated utilizing the Debye Scherrer **Eq.2**.

$$D = \frac{0.9\lambda}{\beta \cos(2\theta)} \qquad \textbf{(2)}$$

Where D is the crystalline size of nanoparticles (nm), λ is the X-ray wavelength (1.5406 Å), β is the full-width at half maximum (FWHM) in radians, and θ is the Bragg angle. Based on the (311) diffraction peak, the average crystallite sizes of Co_3O_4 NPs synthesized utilizing *C. siliquastrum*, Thyme, and *T. oliverianum* extracts were 18.20, 19.74, and 23.39 nm, respectively, compared with 26.82 nm for chemically synthesized Co_3O_4 NPs (**Table 1**). The smaller crystallite sizes of the green-synthesized samples are attributed to peak broadening of the (311) reflection. Additionally, slight shifts in diffraction peak positions were observed among the plant-extract-mediated samples (**Figure 5b**), likely due to variations in the type and concentration of phytochemicals, like flavonoids, phenolic, and tannins [43].

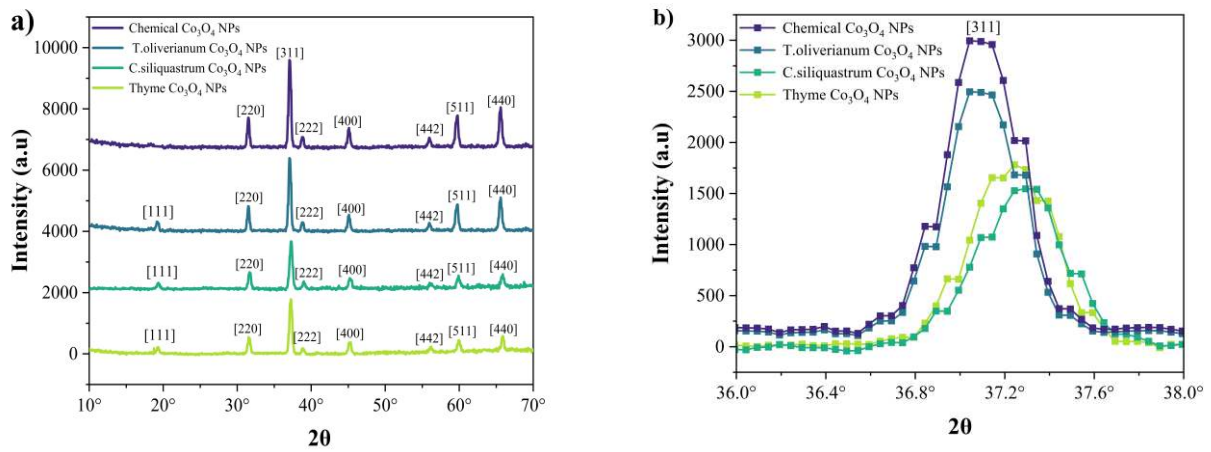

Figure 5. X-ray diffraction and peak diffraction for green and chemically Co_3O_4 NPs. **(a)** Ray diffraction (XRD) pattern and **(b)** diffraction peak.

Table 1. The peak positions of X-ray Diffraction of green and chemically synthesized Co_3O_4 NPs.

Samples	Intensity Peak (311) Position	FWHM β (Degree)	Crystallite Size (nm)	Dislocation Density (δ)	Microstrain (ε)	Crystallinity Index (CI)

Chemical Co_3O_4 NPs	37.010	0.312	26.82	0.001390	0.00408	1.183325
C. siliquastrum Co_3O_4 NPs	37.241	0.461	18.19	0.003023	0.00597	1.096839
T. oliverianum Co_3O_4 NPs	37.068	0.358	23.39	0.001828	0.00467	1.094162
Thyme Co_3O_4 NPs	37.200	0.420	19.74	0.002566	0.00544	1.030747

Abbreviation: FWHM—Full-Width Half Maximum.

3.2. Morphological Analysis

3.2.1. FESEM analysis

The manufactured products are examined utilizing FESEM to investigate the size and morphological characteristics of Co_3O_4 NPs synthesized via both green and chemical methods. FESEM analysis demonstrated that the synthesis route significantly influenced the morphology and particle-size distribution of Co_3O_4 NPs. The Co_3O_4 NPs synthesized utilizing *C. siliquastrum* leaf extract **Figure 6 (a** and **b)** exhibited densely distributed quasi-spherical to slightly polyhedral particles with moderate agglomeration and a narrow particle-size distribution, showing an average size of 19.95 nm, indicating effective nucleation and growth control by plant phytochemicals acting as reducing and capping agents. Similarly, Thyme extract-mediated Co_3O_4 NPs **Figure 6** (**c** and **d**)displayed semi-spherical and irregularly faceted particles with relatively higher aggregation and broader size distribution (20.35 nm), suggesting variations in stabilization efficiency associated with the phytochemical composition of the extract. In contrast, *T. oliverianum*-mediated nanoparticles **Figure 6 (e, f)** showed irregular morphology, pronounced agglomeration, and a wider particle-size distribution with a larger average diameter (25.59 nm), indicating reduced control over crystal growth and particle stabilization. The chemically synthesized Co_3O_4 NPs **Figure 6 (g, h**) exhibited well-defined faceted/polyhedral crystalline morphology and the largest average particle size (31.74 nm), reflecting unrestricted crystal growth in the absence of bioactive capping molecules. Overall, the FESEM results confirm that green synthesis effectively reduced particle size and improved morphological control compared with chemical synthesis. The crystallite size estimated from XRD analysis is notably smaller than the size determined from FESEM images for the corresponding Co_3O_4 NPs samples. This discrepancy arises from the fundamental differences between the two techniques. XRD analysis, based on Debye-Scherrer's equation, provides an estimate of the size of individual crystallographic domains within the sample. In contrast, FESEM analysis measures the overall size of nanoparticles, including their surface morphology and distribution. The larger particle dimensions observed in FESEM images likely indicate that the nanoparticles are composed of multiple crystallographic domains rather than a single domain [44].

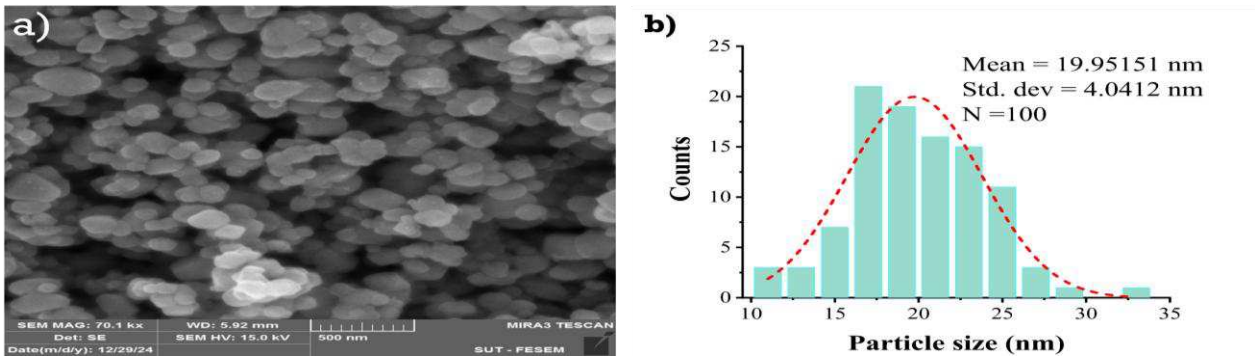

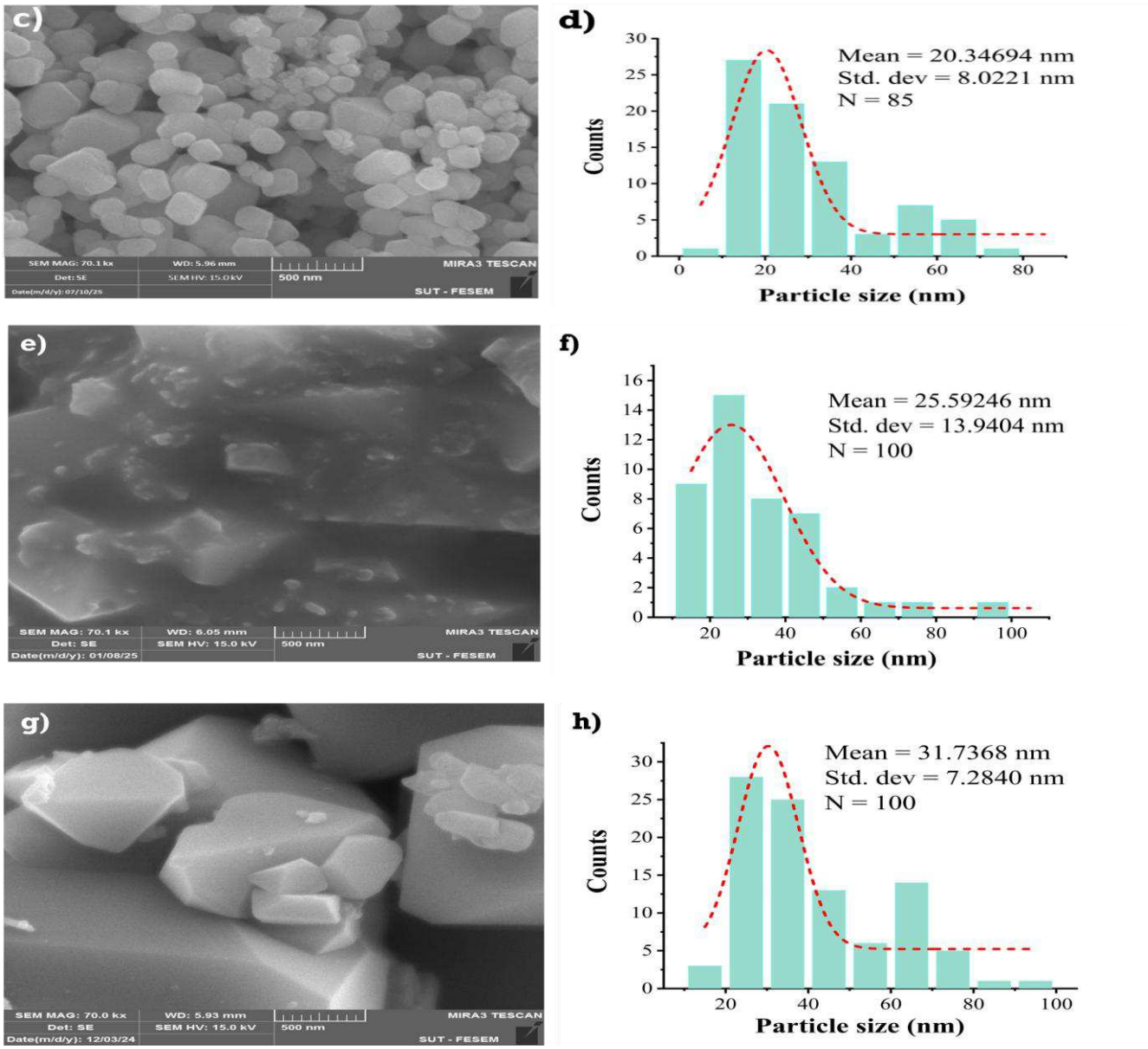

Figure 6. FESEM image of Co_3O_4 NPs preparing utilizing **(a, b)** *C. siliquastrum* leaf extract **(c, d)** Thyme extract **(e, f)** *T. oliverianum* leaf extract, and **(g, h)** chemically Co_3O_4 NPs.

3.2.2. Transmission Electron Microscopy (TEM)

Transmission Electron Microscopy (TEM) characterization demonstrated noticeable differences in both morphology and particle size between green and chemically synthesized Co_3O_4 nanoparticles. The green synthesis approach produced considerably smaller nanoparticles than the conventional chemical method. As illustrated in **Figure 7 (a-e),** the nanoparticles generally exhibited a spherical to near-spherical morphology, with minor agglomeration observed in certain regions. The particle size distribution varied according to the type of plant extract employed during synthesis. the inset histograms associated with each TEM image indicate that nanoparticles synthesized utilizing *C. siliquastrum* leaf extract possessed the smallest average particle size (20 nm), suggesting the presence of highly effective capping and stabilizing compounds. In comparison, nanoparticles prepared with Thyme and *T. oliverianum* extracts displayed average sizes of 21.42 nm and 24.1 nm, respectively. Conversely, the chemically synthesized Co_3O_4 NPs exhibited a significantly

larger mean particle size of approximately 32 nm, as presented in **Figure 7 (g, h)**. The decrease in particle size observed for the green-synthesized nanoparticles can be attributed to the phytochemical constituents present in the plant extracts, which function as both reducing and capping agents. These bioactive compounds regulate the nucleation and growth stages of nanoparticles formation, resulting in smaller, more uniformly distributed particles with improved monodisperse nanoparticles [45].

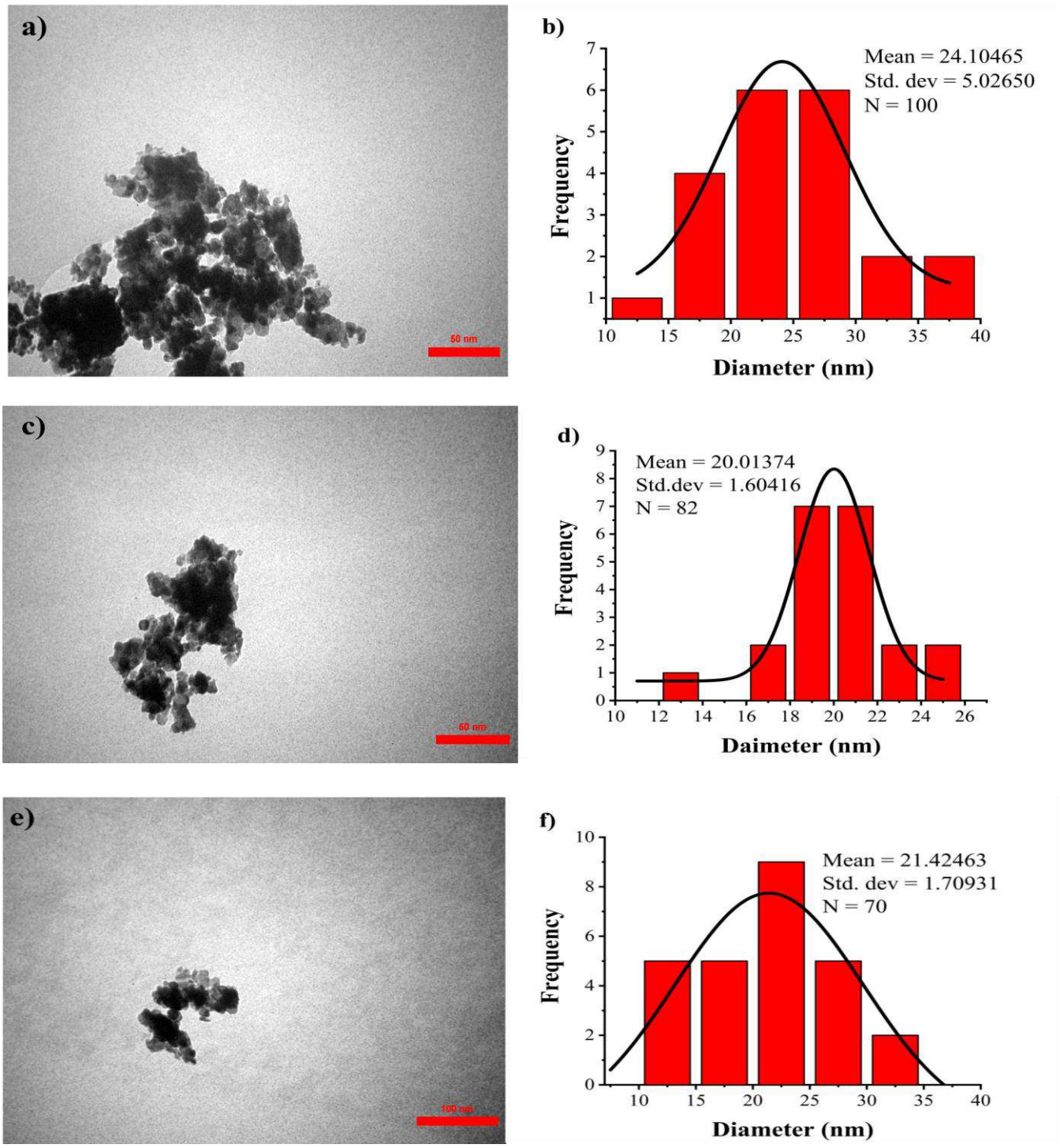

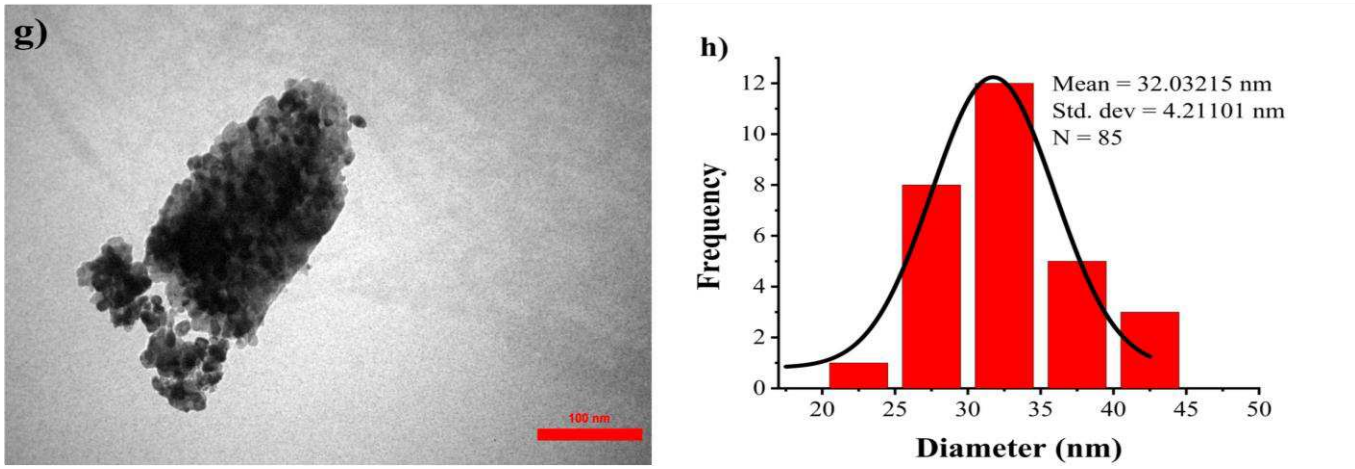

Figure 7. TEM images and histogram size distribution for **(a-b)** *T. oliverianum* Co_3O_4 NPs, **(c-d)** *C. siliquastrum* Co_3O_4 NPs, **(e-f)** Thyme Co_3O_4 NPs, and **(g-h)** Chemically Co_3O_4 NPs.

3.3. Dynamic Light Scattering (DLS)

Complementing the FESEM and TEM findings, we analyze the hydrodynamic size of synthesized Co_3O_4 NPs in aqueous solution using dynamic light scattering (DLS) to gain insights into their colloidal characteristics. It has been noticed that the hydrodynamic size distribution of Co_3O_4 NPs possesses a mean diameter of 75.5 nm, 55.2 nm, 50.2 nm for green and 80.5 nm for the chemical method (***Figure 8***). These hydrodynamic diameters are larger than those observed by FESEM, aligning with observations reported in earlier studies. To assess the surface charge and colloidal stability of the synthesized Co_3O_4 NPs, zeta potential measurements were performed utilizing DLS (see ***Figure 8***). The analysis reveals zeta potential values of -35.7 mV, -55 mV, -60 mV for green-synthesized Co_3O_4 NPs and-30 mV for chemically synthesized Co_3O_4 NPs. Previous studies suggest that nanoparticles with high zeta potential values (with an absolute value greater than 30 mV) generally exhibit high colloidal stability [54]. Accordingly, the observed negative zeta potential values, particularly the more pronounced value for green Co_3O_4 NPs, indicate superior stability of these nanoparticles. This enhanced stability aligns with the smaller hydrodynamic size observed for green-synthesized Co_3O_4 NPs, as particles with less negative zeta potential values are more susceptible to aggregation because of stronger interparticle interactions [46].

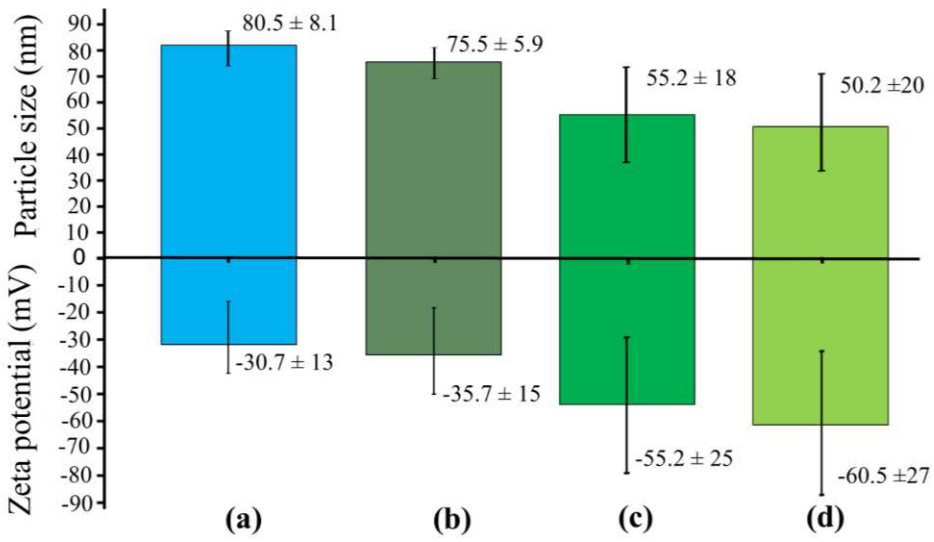

Figure 8. Hydrodynamic size distribution and zeta potential measurement of green and chemically synthesized Co_3O_4 NPs by Dynamic Light Scattering (DLS). **(a)** Chemically **(b)** *T. oliverianum* leaf extract **(c)** Thyme extract and **(d)** *C. siliquastrum* leaf extract.

3.4. Effect of Co_3O_4 NPs on methylene blue (MB) dye degradation

Previous studies have demonstrated that Co_3O_4 NPs exhibit significant photocatalytic activity for the degradation of methylene blue (MB) dye under both UV and visible light irradiation [23][37][28]. In the present work, we investigated the photocatalytic performance of the both green and chemically synthesized Co_3O_4 NPs for the degradation of MB solution under UV light. ***Figure 9*** presents the UV–vis absorption spectra of aqueous MB solution exposed to UV light (< 400 nm) in the presence of Co_3O_4 NPs synthesized utilizing Thyme, *T. oliverianum* and *C. siliquastrum* leaf extracts, as well as chemically synthesized counterpart. For each test, (0.25 - 1.0 g) of Co_3O_4 NPs were add to 20 ml of MB solution (initial concentration: 50 ppm), and the mixture was maintained at 323 K with a stirring speed of 400 rpm for 60 minutes. Initially, we followed the standard protocol by stirring the methylene blue (MB) solution with 0.75g of the Co_3O_4 NPs in the dark for 30 minutes to establish adsorption–desorption equilibrium between the solution and catalyst before irradiation from the 50 W of the UV light. UV-Vis measurements were conducted immediately after the 30 min dark period, these measurements showed only a very minimal decrease in MB concentration, indicating negligible adsorption onto the catalyst surface during this equilibrium step. This confirms that the observed MB degradation during UV exposure is primarily owing to the photocatalytic activity of the synthesized Co_3O_4 NPs, rather than physical adsorption, show in ***Figure 9*** **(a).**

Our results (***Figure 9*** **b**) reveal that both types Co_3O_4 NPs of significantly enhance degradation of methylene blue (MB) dye compared to the MB without NPs (control) at the 0.75 gram. At this concentration, green *C. siliquastrum* Co_3O_4 NPs achieve a degradation percentage of 55.1 %, Thyme Co_3O_4 NPs achieve percentage 52.81 %, and *T. oliverianum* Co_3O_4 NPs 49.76 %, significantly higher than the 46.98 % observed with chemically synthesized Co_3O_4 NPs and the 10.98 % of the control. Based on these findings, 0.75g is determined to be the optimal Co_3O_4 NPs concentration.

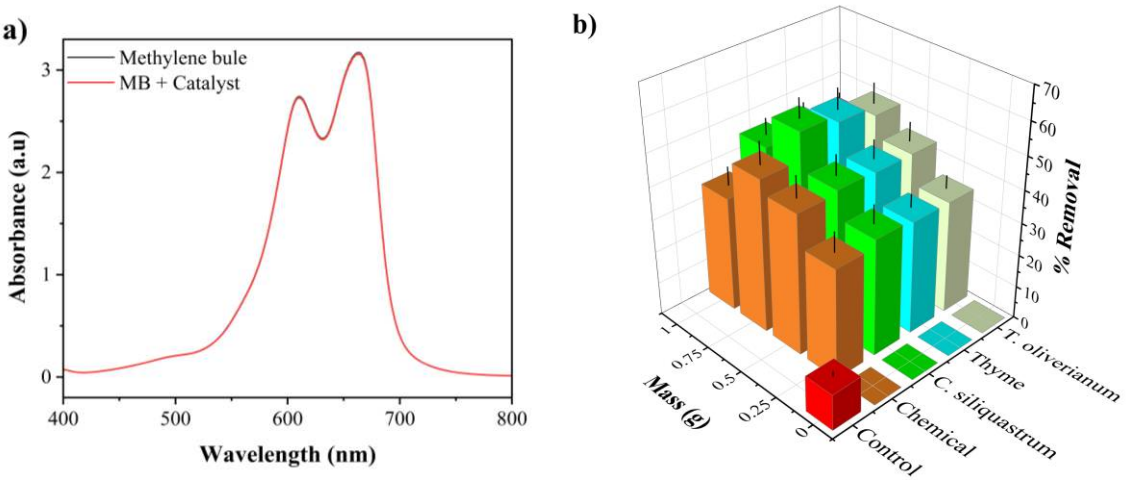

Figure 9. (a) Standard protocol of the MB with catalyst in the dark for 30 min, **(b)** effect of green and chemically synthesized Co_3O_4 NPs on percentage of removal of methylene blue in water. Data are mean ± SD from three independent experiments.

3.5. Effect of time on degradation of the methylene blue (MB) dye

For each experimental run, 0.75 g of Co_3O_4 NPs was dispersed in 20 mL of MB solution with an initial concentration of 50 ppm. The suspension was stirred at 400 rpm and maintained at 323 K for different reaction times ranging from 30 to 240 minutes (30, 60, 90, 120, 150, 180, 210 and 240 min). As illustrated in **Figure 10**, the characteristic absorption peak of MB progressively decreased with increasing irradiation time in the presence of both green-synthesized and chemically synthesize Co_3O_4 NPs, demonstrating their photocatalytic activity relative to the control sample containing only MB solution. A visible reduction in dye color was observed after 30 minutes of UV exposure, while extensive degradation occurred after 240 minutes. According to ***Figure 11***, all Co_3O_4 NPs samples significantly improved MB degradation compared with the control after 240 minutes. The highest degradation efficiency was achieved by Co_3O_4 NPs synthesized *C. siliquastrum* extract, reaching 98.99 %. Nanoparticles prepared from Thyme and *T. oliverianum* extracts showed degradation efficiencies of 95.42 % and 95.30 %, respectively. In contrast, chemically synthesized Co_3O_4 NPs achieved 89.64 % degradation, whereas the control sample exhibited only 25.98 % degradation.

The enhanced photocatalytic performance of the green-synthesized nanoparticles can be attributed to their smaller particle size and the presence of natural phytochemical capping agents derived from *C. siliquastrum*, Thyme, and *T. oliverianum* leaf extracts [47][48]. These characteristics likely increase the surface reactivity of the nanoparticles toward MB molecules, resulting in more efficient dye degradation. the results indicate that green-synthesized Co_3O_4 NPs are promising photocatalysts for the removal of methylene blue from waste water, 0.75 g green Co_3O_4 NPs at 240 min, though field validation remains essential to confirm these controlled-environment results.

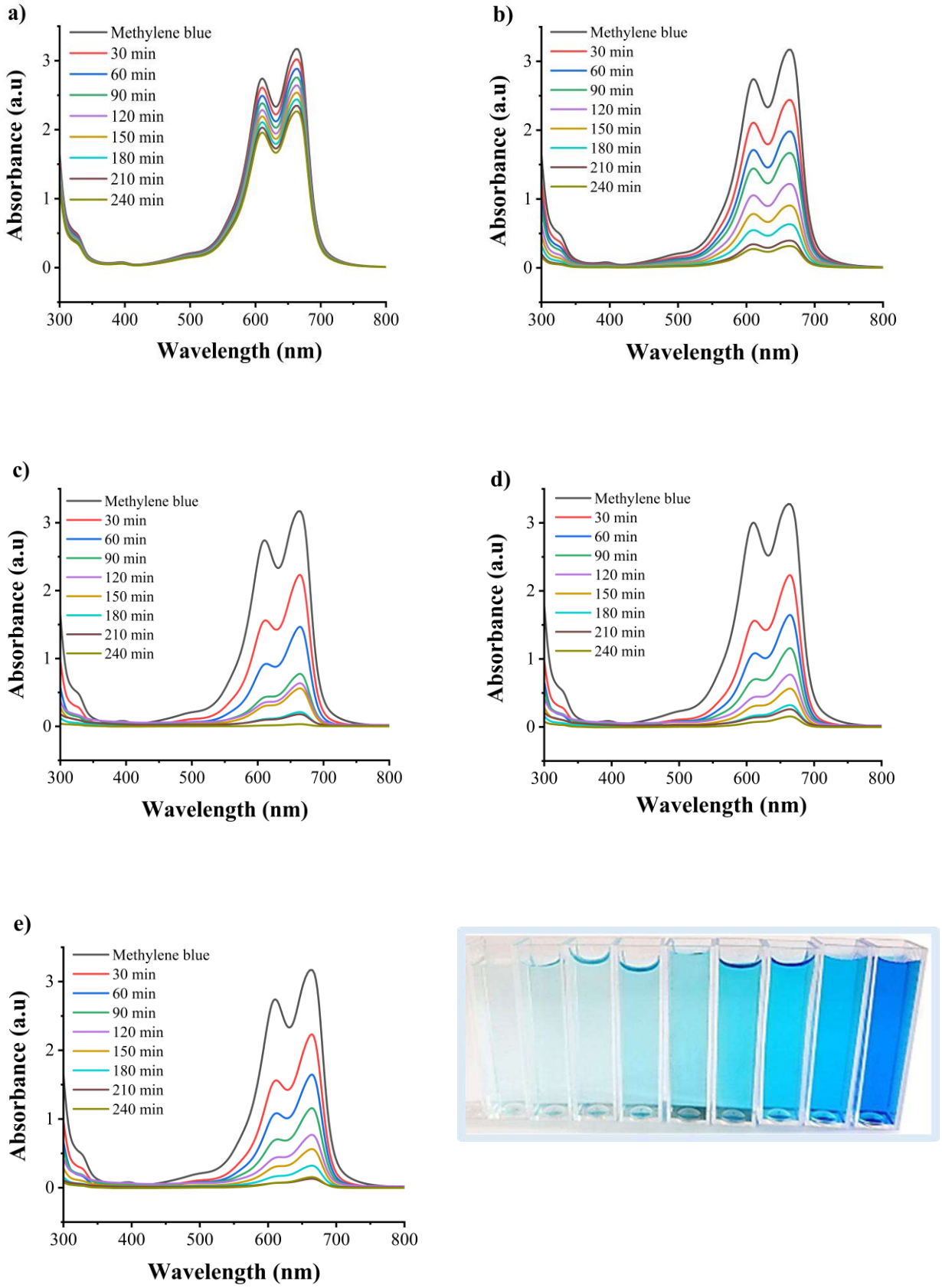

Figure 10. Absorption spectrum for remediation of 50 ppm MB dye utilizing **(a)** control (MB under UV light)**, (b)** chemical Co_3O_4 NPs, **(c)** *C. siliquastrum*, **(d)** Thyme, and **(e)** *T. oliverianum* Co_3O_4 NPs at different time.

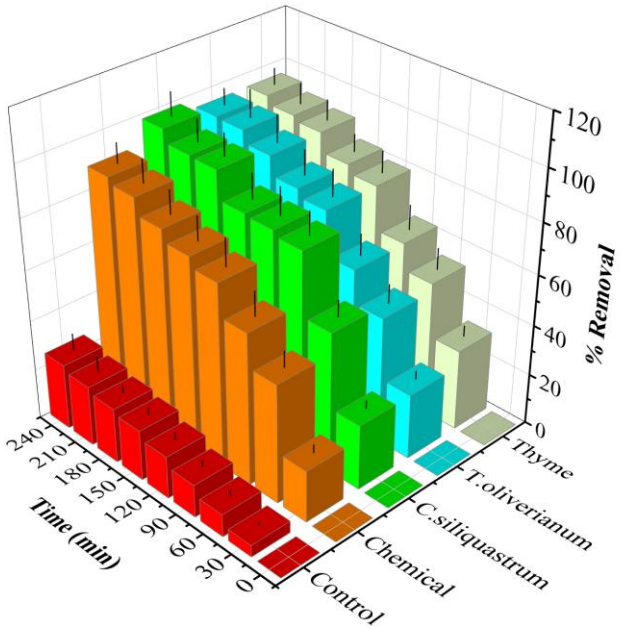

Figure 11. Percent removal of 50 ppm MB dye at different times utilizing green and chemically Co_3O_4 NPs. Data are mean ± SD from three independent experiments.

From ***Figure 11***, Cleary shows that the optimal removal efficiency of MB pigment occurred within 240 minutes of contact time. With balance being reached after 240 minutes, beyond this point, no noticeable change in the colour was detected. through (750 mg) of *T. oliverianum*, Thyme, *C. siliquastrum,* and chemically Co_3O_4 NPs as an adsorbent, at constant 50 ppm concentration for each four cobalt oxide nanoparticles, 98.99 % MB dye removal was accomplished with *C. siliquastrum* Co_3O_4 nanoparticles, 95.42 % with Thyme Co_3O_4NPs, 95.30 % with *T. oliverianum* Co_3O_4 NPs, and 89.64 % with chemically Co_3O_4NPs. The nearly complete disappearance of the peaks at the final stages confirms the successful degradation of MB, making this process a promising approach for wastewater treatment application. After photocatalytic degradation of methylene blue dye under UV light, the concentration of cobalt ions (Co^{2+}) leached into the solution was analyzed by ICP-OES for each catalyst. The results are summarized in **Table 2.**

Table 2. The result summarized the concentration Co^{2+} ion leaching into solution each catalyst.

Samples	**ICP-OES**		
	Co^{2+} leaching (mg/L)	**Observation**	**Reproducibility**
Chemical Co_3O_4 NPs	1.21	Moderate leaching; large particle size	<1%
C.siliquastrum Co_3O_4 NPs	0.32	Low leaching; stable structure	
T.oliverianum Co_3O_4 NPs	0.78	Acceptable leaching; relatively	
Thyme Co_3O_4 NPs	0.41	Low leaching; good stability	

When UV light initiates is a chemical process in which an organic compound splits into simpler, harmless molecules and Co_3O_4 NPs degrade photocatalytically. The decomposition of the chromophoric group and transformation of the dye into low molecular-weight products are associated with this process [49][50]. When exposed to radiation, the catalyst surface produces electrons and holes (e & h^+), which is the primary cause of the dye degradation [51]. The water molecule joins the hole created by the dye degradation and transforms it into an OH radical, while the O_2 scavenges the electron and transforms it into OH via the intermediates of HOO and H_2O_2. Strong oxidizing agents like OH break down dyes non-selectively into water, carbon dioxide, and inorganic ions [52]. Following their reaction with organic molecules, such as pollutants or toxins, these reactive oxygen species can decompose them into smaller, less dangerous substances like H_2O and carbon dioxide. The results demonstrate that the MB dye adsorption mechanism relies on simple adsorbed through the photocatalytic activity of Co_3O_4 under Ultraviolet light in ***Figure 12***.

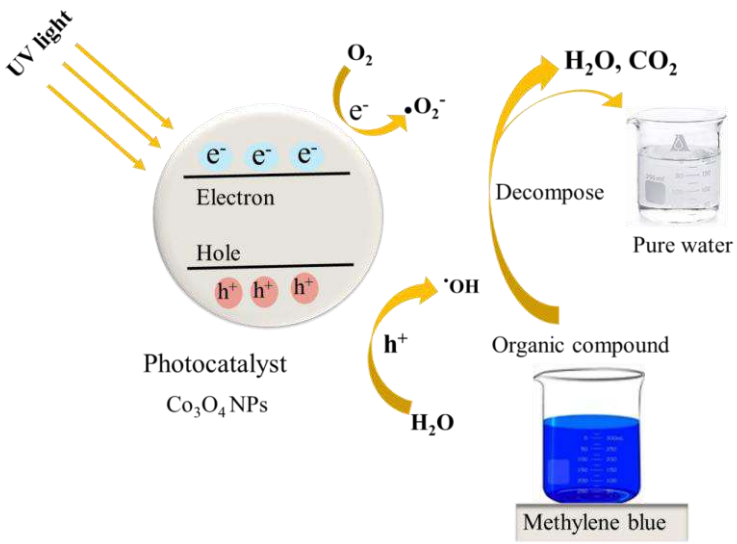

Figure 12. Mechanism of photocatalytic degradation methylene blue (MB) under Ultraviolet light.

4. Conclusion

This study demonstrated the successful green synthesis of cobalt oxide nanoparticles (Co_3O_4 NPs) using leaf extracts of *Teucrium oliverianum*, *Thymus vulgaris* (thyme), and *Cercis siliquastrum*. The synthesized nanoparticles were characterized using UV–Vis spectroscopy, FTIR, XRD, FE-SEM, EDX, and TEM, confirming the formation of crystalline Co_3O_4 nanoparticles with favorable structural and morphological properties. Compared with the conventional chemical method, the green synthesis approach produced smaller and more uniformly distributed nanoparticles, highlighting the important role of plant-derived phytochemicals as natural reducing and stabilizing agents.The photocatalytic performance of the synthesized nanoparticles was evaluated through the degradation of methylene blue under UV irradiation. The green-synthesized Co_3O_4 nanoparticles exhibited superior photocatalytic activity compared with chemically synthesized nanoparticles and the catalyst-free system, demonstrating the effectiveness of plant-mediated synthesis in enhancing photocatalytic efficiency. Among the investigated plant extracts, *Cercis siliquastrum* produced the most effective photocatalyst, indicating that the phytochemical composition of the extract plays an important role in determining nanoparticle properties and catalytic performance.Overall, this work highlights green synthesis as a simple, sustainable, and environmentally friendly strategy for producing efficient Co_3O_4 photocatalysts for wastewater treatment.

The excellent photocatalytic activity, combined with the low cost and eco-friendly nature of the synthesis process, suggests considerable potential for treating dye-contaminated industrial wastewater. Future studies should focus on catalyst reusability, long-term stability, large-scale applications, and environmental safety to facilitate practical implementation.

Acknowledgement: The authors are appreciative of the Salahaddin University-Erbil and University of Garmian for supporting this research.

Data Availability: the data supporting the study's findings will be made available by the corresponding author upon reasonable request.

Declarations

Conflict of interest the authors declare no conflicts of interest.

Reference

[1] D. Bouras, M. Fellah, A. Mecif, R. Barillé, A. Obrosov, and M. Rasheed, "High photocatalytic capacity of porous ceramic-based powder doped with MgO," *J. Korean Ceram. Soc.*, vol. 60, no. 1, pp. 155–168, 2023.

[2] S. Riaz *et al.*, "Bactericidal action and industrial dye degradation of graphene oxide and polyacrylic acid-doped SnO2 quantum dots: In silico molecular docking study," *ACS omega*, vol. 8, no. 6, pp. 5808–5819, 2023.

[3] A. Rafiq, M. Imran, M. Aqeel, M. Naz, M. Ikram, and S. Ali, "Study of transition metal ion doped CdS nanoparticles for removal of dye from textile wastewater," *J. Inorg. Organomet. Polym. Mater.*, vol. 30, pp. 1915–1923, 2020.

[4] R. N. Bharagava, G. Saxena, and S. I. Mulla, "Introduction to industrial wastes containing organic and inorganic pollutants and bioremediation approaches for environmental management," *Bioremediation Ind. Waste Environ. Saf. Vol. I Ind. Waste Its Manag.*, pp. 1–18, 2020.

[5] A. Ansari *et al.*, "Green synthesis of TiO2 nanoparticles using Acorus calamus leaf extract and evaluating its photocatalytic and in vitro antimicrobial activity," *Catalysts*, vol. 12, no. 2, p. 181, 2022.

[6] S. Thakur and M. S. Chauhan, "Treatment of dye wastewater from textile industry by electrocoagulation and Fenton oxidation: a review," *Water Qual. Manag. Sel. Proc. ICWEES-2016*, pp. 117–129, 2018.

[7] D. Bouras, M. Rasheed, R. Barille, and M. N. Aldaraji, "Efficiency of adding DD3+ (Li/Mg) composite to plants and their fibers during the process of filtering solutions of toxic organic dyes," *Opt. Mater. (Amst).*, vol. 131, p. 112725, 2022.

[8] F. Lu and D. Astruc, "Nanocatalysts and other nanomaterials for water remediation from organic pollutants," *Coord. Chem. Rev.*, vol. 408, p. 213180, 2020.

[9] F. Uddin, "Environmental hazard in textile dyeing wastewater from local textile industry," *Cellulose*, vol. 28, no. 17, pp. 10715–10739, 2021.

[10] P. Nuengmatcha, S. Chanthai, R. Mahachai, and W.-C. Oh, "Sonocatalytic performance of ZnO/graphene/TiO2 nanocomposite for degradation of dye pollutants (methylene blue, texbrite BAC-L, texbrite BBU-L and texbrite NFW-L) under ultrasonic irradiation," *Dye. Pigment.*, vol. 134, pp. 487–497, 2016.

[11] R. Salami, M. Amini, M. Bagherzadeh, and H. Hosseini, "Vanadium supported on spinel cobalt ferrite nanoparticles as an efficient and magnetically recoverable catalyst for oxidative degradation of methylene blue," *Appl. Organomet. Chem.*, vol. 33, no. 10, p. e5127, 2019.

[12] M. M. Higgins, M. T. González, and J. Rojas, "Enhanced X-RAYS degradation of methylene blue in the presence of gold microspheres," *Radiat. Phys. Chem.*, vol. 156, pp. 73–80, 2019.

[13] T. N. J. I. Edison, R. Atchudan, C. Kamal, and Y. R. Lee, "Caulerpa racemosa: a marine green alga for eco-friendly synthesis of silver nanoparticles and its catalytic degradation of methylene blue," *Bioprocess Biosyst. Eng.*, vol. 39, pp. 1401–1408, 2016.

[14] E. Brillas and C. A. Martínez-Huitle, “Decontamination of wastewaters containing synthetic organic dyes by electrochemical methods. An updated review,” *Appl. Catal. B Environ.*, vol. 166, pp. 603–643, 2015.

[15] Z. Z. Vasiljevic *et al.*, “Photocatalytic degradation of methylene blue under natural sunlight using iron titanate nanoparticles prepared by a modified sol–gel method,” *R. Soc. open Sci.*, vol. 7, no. 9, p. 200708, 2020.

[16] S. M. Tichapondwa, J. P. Newman, and O. Kubheka, “Effect of TiO2 phase on the photocatalytic degradation of methylene blue dye,” *Phys. Chem. Earth, Parts A/B/C*, vol. 118, p. 102900, 2020.

[17] M. Cheng *et al.*, “Hydroxyl radicals based advanced oxidation processes (AOPs) for remediation of soils contaminated with organic compounds: a review,” *Chem. Eng. J.*, vol. 284, pp. 582–598, 2016.

[18] S. H. S. Chan, T. Yeong Wu, J. C. Juan, and C. Y. Teh, “Recent developments of metal oxide semiconductors as photocatalysts in advanced oxidation processes (AOPs) for treatment of dye waste-water,” *J. Chem. Technol. Biotechnol.*, vol. 86, no. 9, pp. 1130–1158, 2011.

[19] U. D. Babar *et al.*, “Study the photovoltaic performance of pure and Cd-doped ZnO nanoparticles prepared by reflux method,” *Mater. Today Proc.*, vol. 43, pp. 2780–2785, 2021.

[20] S. Shamaila, A. K. L. Sajjad, S. A. Farooqi, N. Jabeen, S. Majeed, and I. Farooq, “Advancements in nanoparticle fabrication by hazard free eco-friendly green routes,” *Appl. Mater. Today*, vol. 5, pp. 150–199, 2016.

[21] M. A. Hanif, Y.-S. Kim, J. Akter, H. G. Kim, and L. K. Kwac, “Fabrication of robust and stable N-doped ZnO/single-walled carbon nanotubes: characterization, photocatalytic application, kinetics, degradation products, and toxicity analysis,” *ACS omega*, vol. 8, no. 18, pp. 16174–16185, 2023.

[22] O. A. A. El-Shamy and M. A. Deyab, “The most popular and effective synthesis processes for Co3O4 nanoparticles and their benefit in preventing corrosion,” *Zeitschrift für Phys. Chemie*, vol. 237, no. 3, pp. 333–350, 2023.

[23] A. Heydari, Z. Gardner, X. Luo, B. M. Alotaibi, A. Motamedisade, and C. L. Raston, “Methylene blue degradation using vortex fluidic device under UV irradiation: Comparison of response surface methodology and artificial neural network,” *Environ. Technol. Innov.*, vol. 38, no. March, p. 104127, 2025, doi: 10.1016/j.eti.2025.104127.

[24] V. N. Sonkusare *et al.*, “Mesoporous octahedron-shaped tricobalt tetroxide nanoparticles for photocatalytic degradation of toxic dyes,” *ACS omega*, vol. 5, no. 14, pp. 7823–7835, 2020.

[25] K. Hkiri, H. E. A. Mohamed, M. Ben Salem, A. Kouki, M. Maaza, and M. Zouaoui, “Biosynthesis and characterization of CaZrO 3 nanoparticles via hyphaene thebaica: Effect of preparation method on morphology, electrical, and dielectric properties,” *J. Mater. Sci. Mater. Electron.*, vol. 31, pp. 10018–10030, 2020.

[26] Z. U. H. Khan *et al.*, “Biomedical applications of green synthesized Nobel metal nanoparticles,” *J. Photochem. Photobiol. B Biol.*, vol. 173, pp. 150–164, 2017.

[27] V. Ratchagar *et al.*, “Coprecipitation Methodology Synthesis of Cobalt-Oxide Nanomaterials Influenced by pH Conditions: Opportunities in Optoelectronic Applications,” *Int. J. Photoenergy*, vol. 2023, no. 1, p. 2493231, 2023.

[28] A. Safdar, H. E. A. Mohamed, K. Hkiri, A. Muhaymin, and M. Maaza, “Green Synthesis of Cobalt Oxide Nanoparticles Using Hyphaene thebaica Fruit Extract and Their Photocatalytic Application,” *Appl. Sci.*, vol. 13, no. 16, 2023, doi: 10.3390/app13169082.

[29] S. Thota, A. Kumar, and J. Kumar, “Optical, electrical and magnetic properties of Co3O4 nanocrystallites obtained by thermal decomposition of sol–gel derived oxalates,” *Mater. Sci. Eng. B*, vol. 164, no. 1, pp. 30–37, 2009.

[30] D. Anggraini, P. K. Wardani, M. Agustina, A. Awaluddin, and K. Arifin, “Tio2/Co3O4 composite as photoanode of photoelectrochemical water splitting,” in *Journal of Physics: Conference Series*, IOP Publishing, 2019, p. 12032.

[31] C. T. Anuradha and P. Raji, “Facile synthesis and characterization of Co3O4 nanoparticles for high-performance supercapacitors using Camellia sinensis,” *Appl. Phys. A*, vol. 126, no. 3, p. 164, 2020.

[32] T. He, D. Chen, X. Jiao, Y. Wang, and Y. Duan, “Solubility-controlled synthesis of high-quality Co3O4 nanocrystals,” *Chem. Mater.*, vol. 17, no. 15, pp. 4023–4030, 2005.

[33] A. B. Vennela, D. Mangalaraj, N. Muthukumarasamy, S. Agilan, and K. V Hemalatha, "Structural and optical properties of Co3O4 nanoparticles prepared by sol-gel technique for photocatalytic application," *Int. J. Electrochem. Sci.*, vol. 14, no. 4, pp. 3535–3552, 2019.

[34] F. Faghihzadeh, N. M. Anaya, L. A. Schifman, and V. Oyanedel-Craver, "Fourier transform infrared spectroscopy to assess molecular-level changes in microorganisms exposed to nanoparticles," *Nanotechnol. Environ. Eng.*, vol. 1, pp. 1–16, 2016.

[35] T. S. Gaaz, A. B. Sulong, A. A. H. Kadhum, A. A. Al-Amiery, M. H. Nassir, and A. H. Jaaz, "The impact of halloysite on the thermo-mechanical properties of polymer composites," *Molecules*, vol. 22, no. 5, p. 838, 2017.

[36] I. Bibi *et al.*, "Green and eco-friendly synthesis of cobalt-oxide nanoparticle: characterization and photo-catalytic activity," *Adv. Powder Technol.*, vol. 28, no. 9, pp. 2035–2043, 2017.

[37] R. Bhargava, S. Khan, N. Ahmad, and M. M. N. Ansari, "Investigation of structural, optical and electrical properties of Co3O4 nanoparticles," in *AIP conference proceedings*, AIP Publishing, 2018.

[38] R. Govindasamy *et al.*, "Green Synthesis and Characterization of Cobalt Oxide Nanoparticles Using Psidium guajava Leaves Extracts and Their Photocatalytic and Biological Activities," *Molecules*, vol. 27, no. 17, pp. 1–16, 2022, doi: 10.3390/molecules27175646.

[39] V. D. Rajeswari, A. S. Khalifa, A. Elfasakhany, I. A. Badruddin, S. Kamangar, and K. Brindhadevi, "Green and ecofriendly synthesis of cobalt oxide nanoparticles using Phoenix dactylifera L: Antimicrobial and photocatalytic activity," *Appl. Nanosci.*, vol. 13, no. 2, pp. 1367–1375, 2023.

[40] J. Feng and H. C. Zeng, "Size-controlled growth of Co3O4 nanocubes," *Chem. Mater.*, vol. 15, no. 14, pp. 2829–2835, 2003.

[41] S.-H. Wu and D.-H. Chen, "Synthesis and characterization of nickel nanoparticles by hydrazine reduction in ethylene glycol," *J. Colloid Interface Sci.*, vol. 259, no. 2, pp. 282–286, 2003.

[42] M. R. S. A. Janjua, "Synthesis of Co3O4 nano aggregates by Co-precipitation method and its catalytic and fuel additive applications," *Open Chem.*, vol. 17, no. 1, pp. 865–873, 2019.

[43] S. A. Memon, D. Hassan, J. A. Buledi, A. R. Solangi, S. Q. Memon, and I. M. Palabiyik, "Plant material protected cobalt oxide nanoparticles: sensitive electro-catalyst for tramadol detection," *Microchem. J.*, vol. 159, p. 105480, 2020.

[44] R. N. Aljawfi, M. J. Alam, F. Rahman, S. Ahmad, A. Shahee, and S. Kumar, "Impact of annealing on the structural and optical properties of ZnO nanoparticles and tracing the formation of clusters via DFT calculation," *Arab. J. Chem.*, vol. 13, no. 1, pp. 2207–2218, 2020.

[45] B. Avinash *et al.*, " Green-synthesised cobalt oxide (Co 3 O 4) nanoparticles using aloe-vera latex for their photocatalytic and electrochemical sensor studies ," *Sens. Technol.*, vol. 1, no. 1, p., 2023, doi: 10.1080/28361466.2023.2286948.

[46] A. Brunelli *et al.*, "Colloidal stability classification of TiO2 nanoparticles in artificial and in natural waters by cluster analysis and a global stability index: Influence of standard and natural colloidal particles," *Sci. Total Environ.*, vol. 829, p. 154658, 2022.

[47] D. J. Pochapski, C. Carvalho dos Santos, G. W. Leite, S. H. Pulcinelli, and C. V. Santilli, "Zeta potential and colloidal stability predictions for inorganic nanoparticle dispersions: Effects of experimental conditions and electrokinetic models on the interpretation of results," *Langmuir*, vol. 37, no. 45, pp. 13379–13389, 2021.

[48] R. Govindasamy *et al.*, "Green synthesis and characterization of cobalt oxide nanoparticles using Psidium guajava leaves extracts and their photocatalytic and biological activities," *Molecules*, vol. 27, no. 17, p. 5646, 2022.

[49] A. Safdar, H. E. A. Mohamed, K. Hkiri, A. Muhaymin, and M. Maaza, "Green synthesis of cobalt oxide nanoparticles using hyphaene thebaica fruit extract and their photocatalytic application," *Appl. Sci.*, vol. 13, no. 16, p. 9082, 2023.

[50] N. T. Nguyen and V. A. Nguyen, "Synthesis, characterization, and photocatalytic activity of ZnO nanomaterials prepared by a green, nonchemical route," *J. Nanomater.*, vol. 2020, no. 1, p. 1768371, 2020.

[51] Y. K. Ashar *et al.*, "Effects of compassion meditation on a psychological model of charitable donation.," *Emotion*, vol. 16, no. 5, p. 691, 2016.

[52] M. Iqbal and I. A. Bhatti, “Gamma radiation/H2O2 treatment of a nonylphenol ethoxylates: degradation, cytotoxicity, and mutagenicity evaluation,” *J. Hazard. Mater.*, vol. 299, pp. 351–360, 2015.